Materials Research Proceedings 28 (2023) 1703-1710 https://doi.org/10.21741/9781644902479-184

Surface topography investigation during nanosecond pulsed laser engraving of SAE304 stainless steel

NIKOLIDAKIS Evangelos[1,a], KARMIRIS-OBRATAŃSKI Panagiotis[2,3,b *], PAPAZOGLOU Emmanouil-Lazaros[3,c], KARKALOS E. Nikolaos[3,d], MARKOPOULOS P. Angelos[3,e] and ANTONIADIS Aristomenis[1,f]

[1]Technical University of Crete, School of Production Engineering & Management, Micromachining & Manufacturing Modeling Laboratory, University campus, Building E4.026-Kounoupidiana, 73100 Chania, Greece

[2]AGH University of Science and Technology, Faculty of Mechanical Engineering and Robotics, Department of Manufacturing Systems, al. Mickiewicza 30, 30-059 Cracow, Poland

[3]National Technical University of Athens, School of Mechanical Engineering, Laboratory of Manufacturing Technology, Heroon Polytechniou 9, 15780, Athens, Greece

[a]krhthkournas@gmail.com, [b]karmiris@agh.edu.pl, [c]mlpapazoglou@gmail.com, [d]nkark@mail.ntua.gr, [e]amark@mail.ntua.gr, [f]aantoniadis@tuc.gr

Keywords: Surface Topography, Laser Engraving, Nanosecond Pulsed Laser, SAE304 Steel

Abstract. Laser engraving process is widely used for various industrial applications, such as the creation of small and complex geometries with ultra-high precision. As surface topography can affect the functionality of produced surfaces in various ways, it is required to carry out comprehensive experimental work in order to correlate the laser engraving process parameters with surface topography characteristics. In the current paper, the surface topography of SAE304 stainless steel specimens in respect to laser power, scanning speed and pulse repetition rate is studied through microscope observations. The findings indicate that the scanning speed is the most dominant parameter regarding surface roughness and from the viewpoint of surface quality, it is suggested that higher scanning speed, lower power and pulse repetition rate values should be employed.

Introduction

Laser machining and laser assisted machining are a rapidly growing non-conventional manufacturing processes class, with lasers becoming gradually more and more significant as part of the modern industrial environment [1]. In general, by the interaction of the material with the laser beam, the material's electrons absorb a proportion of the laser beam energy and become excited [2]. The temperature of the excited electrons sub-system is raised and subsequently the absorbed energy is transferred to the material's atomic lattice, causing it to heat up until its melting and/or ablation. The high energy densities that are employed during laser-based processes provide a number of significant advantages over the conventional machining that include the potential to create small and complex geometries with ultra-high precision, the reduction of the Heat Affected Zone (HAZ), and the deformations due to the thermal and mechanical stress concentration [3]. Laser engraving consists one of the most widely employed laser-based processes.

In laser engraving, the material is removed layer by layer subsequent to the multiple passes of the laser beam over the material surface. Given that usually, in laser engraving, pulsed lasers are utilized, each layer of material is removed by the overlap of the generated craters that are formed due to material ablation [4]. As it was aforementioned, pulsed lasers are most commonly utilized since, although they have lower nominal power, through their pulsed operation extremely high-

power peak and power density can be achieved [5]. In laser engraving, minimum power density of 10^8 W/cm^2 is required and laser pulse durations in the order of nanoseconds are usually utilized. Finally, the operation wavelength of the laser is also an important parameter, since the material reflectivity is directly related with the laser beam wavelength, and thus, the proper type of laser has to be used for each class of material. Hence, neodymium-doped yttrium aluminum garnet Nd:YAG lasers have prevailed over other types of lasers (e.g., CO_2 lasers) for the engraving of metallic materials since the reflectivity of metals in wavelengths around 1064 nm is significantly lower, in comparison with the reflectivity in the range of 10.6 μm wavelengths where CO_2 lasers operate.

The relevant field of laser machining, including the laser engraving, is an area of active research. The laser milling of aluminum-magnesium alloy has been studied by Campanelli et al. [6] in terms of the material removal depth and the surface roughness as function of the machining parameters. Orazi et al. [7] presented a semi-empirical model regarding the Material Removal Rate (MRR) in machining of aluminum alloy 7075 and mild steel AISI 1040 with fiber pulsed laser. Teixidor et al. [8] studied the surface quality and the dimensional accuracy in respect to the process parameters in laser milling of hardened AISI H13 tool steel. In the work of Campaneli et al. [9], an experimental investigation regarding the laser milling of aluminum alloy 5754 was carried out, where the impact of machining parameters on the material removal depth, the MRR and the mean surface roughness Ra was mainly studied. The deep engraving process of AISI 1045 stainless steel was investigated by Anita Pritam [10], with the engraving depth and the surface roughness being the machining process evaluation indexes. The experimental work of Sugar et al. [11] presents a study regarding the effect of machining parameters on the surface quality of laser processed brass. The machinability of titanium alloy Ti6Al4V with laser milling has been investigated in the work of Ahmed et al. [12], with the MRR and the surface roughness being considered as representative indexes of the alloy's machinability. The MRR and the dimensional accuracy in fabrication of microchannels with Nd:YAG laser on alumina was studied by Mohammed et al. [13], while the machining quality of microchannels on Nickel-Titanium (NiTi) based shape-memory alloys was discussed in the work of Mohammed et al. [14]. From the literature review, the importance and interest on studying the surface quality after laser machining and engraving for different materials and alloys is clearly deduced.

The current paper pertains to the surface topography of SAE 304 stainless steel after its engraving with pulsed Nd:YAG laser. From the literature review it is concluded that laser engraving process is very sensitive to the machining parameters, thus, an extensive and detailed study of how each parameter affects the surface topography is scientifically interesting, but also with practical value. Hence, different laser powers, scanning speeds and repetition rates were utilized in order to cover a wide range of machining conditions and define the impact of each parameter on the surface topography. The Design of Experiment (DOE) was based on Taguchi L9 orthogonal array with three factors at three levels each. More specifically, laser power values of 8, 12 and 16 W were used, as well as scanning speed values of 200, 400 and 600 mm/min and pulse repetition rate values of 30, 50 and 70 kHz. Finally, although commonly the surface topography is evaluated based on the Ra and Rz values, in the current study the analysis of surface topography was done in terms of Sa and Sz, while statistical analysis was followed in order the obtained results to be interpreted.

Materials and Methods

The current series of experiments was carried out on a LASERTEC 40 laser machining center made by DMG MORI, which is equipped with a Nd:YAG pulsed laser that operates in 1064 nm wavelength, with 20W maximum nominal average power, nominal spot diameter of 30 μm and 100 ns pulse duration. A stainless steel SAE304 plate of 5 mm thickness was utilized as workpiece. Square pockets of 4x4 mm dimension were engraved by using unidirectional cross hatching

scanning strategy. The track distance T_d, i.e., the distance between two successive tracks was set equal to the hatching distance H_d, i.e., the distance between two subsequent pulses. The hatch distance is calculated based on Eq. 1 and the overlap between the pulses according to Eq. 2.

$$H_d = \frac{v_{scan}}{f} \tag{1}$$

$$overlap = 1 - \frac{H_d}{D} \tag{2}$$

with H_d the hatching distance in [mm], v_{scan} the laser beam scanning speed in [mm/s], D the nominal laser beam diameter and f the repetition rate in [Hz]. The scanning strategy and its main geometrical features are schematically depicted in Fig. 1.

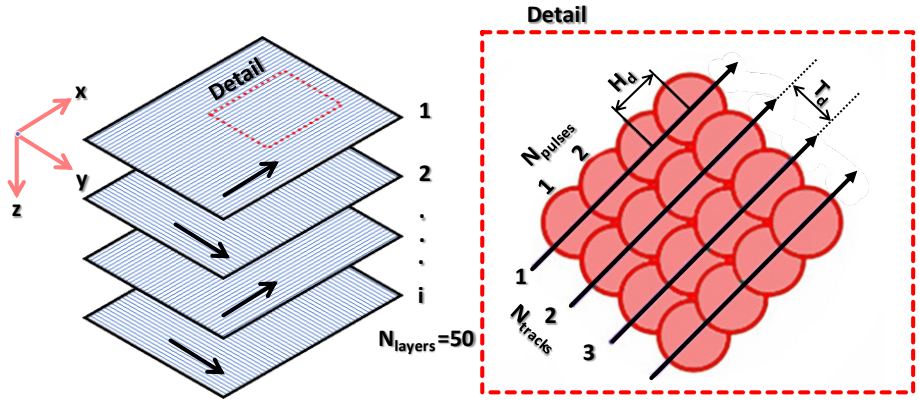

Fig. 1. Unidirectional cross hatching scanning strategy and its main geometrical features.

The DoE was based on Taguchi L9 orthogonal array with three factors at three levels each. Namely, the control parameters were the mean power P, the scanning speed v_{scan} and the repetition rate f. The mean power values were set between 8 and 16 W, the scanning speeds between 200 and 600 mm/s, while the repetition rate took values between 30 and 70 kHz. By utilizing the aforementioned machining parameters, the study covers a wide range of different power densities, hatching distances and track distances, thus, the impact and the significance of each parameter can be assessed. Moreover, in order the process to reach a steady state that will ensure representative and reliable results, each pocket was engraved by 50 successive layers. Finally, by using the touch probe measuring system of the laser machine, the laser beam was initially focused on the top surface of the plate. Thus, the standoff distance was initially zero for the first layer to be engraved, while, for the next layers, the standoff distance was increasing and was equal to the engraving depth. It is worth noting that the maximum applicable engraving depth is almost negligible in relation to the focal length. The machining parameters combinations based on the aforementioned DOE, along with the machining center features are listed in detail in Table 1.

Finally, the study of the surface topography was carried out in terms of Sa and Sz that were defined as:

$$\boldsymbol{Sa} = \frac{\mathbf{1}}{\boldsymbol{A}} \iint_{\boldsymbol{A}} |\boldsymbol{z}(\boldsymbol{x},\boldsymbol{y})|\, dxdy \tag{3}$$

where, A the definition area, and z (x,y) the height of the scale-limited surface at position (x,y) and **Sz** the sum of the largest peak height value and the largest pit height value within a definition area.

The surface roughness values were measured by utilizing the Focus Variation method in a Keyence VHX-7000 optical microscope equipped with specialized lenses. The measurements were

Materials Research Proceedings 28 (2023) 1703-1710 https://doi.org/10.21741/9781644902479-184

conducted by following the ISO 25178-2 standards, while, based on the obtained SR values, the cut off length was defined at 0.8 mm.

Table 1. Machining parameters.

Machining Parameters			
Control Parameters			
#	**Power [W]**	**Scanning Speed [mm/s]**	**Repetition Rate [kHz]**
1	8	200	30
2	8	400	50
3	8	600	70
4	12	200	50
5	12	400	70
6	12	600	30
7	16	200	70
8	16	400	30
9	16	600	50
Constant Parameters			
Spot Size		30 [μm]	
Pulse Duration		100 [ns]	
Number of Layers		50	

Results and Discussion

After the experiments were conducted, the surface topography was investigated by means of Focus Variation microscope. In Fig. 2a and b, the topography of two indicative surfaces produced by laser engraving under two different conditions, namely no.3 and 4, is depicted and in Table 2, the results regarding Sa and Sz are presented for all experiments. From these figures it can be seen that the surface includes various characteristic features, such as craters and peaks due to the intense thermal phenomena induced by the laser beam. Although different process conditions lead to different surface quality, as can be seen from the results of Table 2, this typical morphology is not considerably altered. It is worth noting that this type of surface is similar to the surface produced by other non-conventional processes which involve a high heat input, such as EDM. Although the surface quality is moderate-to-high, with Sa mostly varying between 0.57-1.75 μm, the high values of Sa and Sz observed for the experiments no.4 and 7 can be explained as a result of both high interaction time due to relatively lower value of scanning speed and considerably high overlap values.

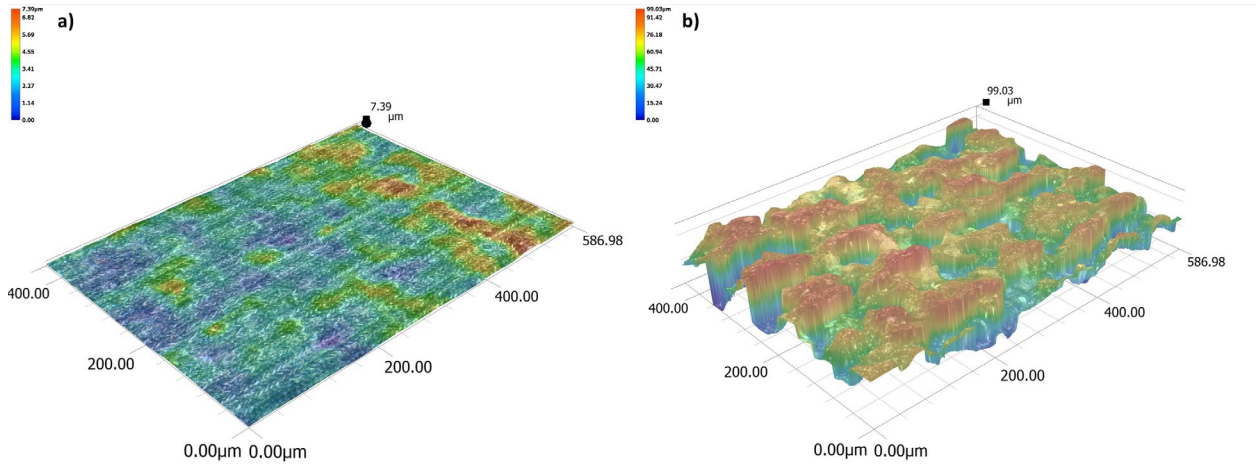

Fig. 2. Surface topography under different process conditions: a) 8 W / 600 mm/s / 70 kHz and b)12 W / 200 mm/s / 50 kHz.

Table 2. Experimental results.

#	Power [W]	Scanning Speed [mm/s]	Repetition Rate [kHz]	Hatching Distance [µm]	Overlap	Sa [µm]	Sz [µm]
1	8	200	30	6.67	0.778	1.75	16.37
2	8	400	50	8.00	0.733	0.84	6.28
3	8	600	70	8.57	0.714	0.57	5.34
4	12	200	50	4.00	0.867	11.57	87.35
5	12	400	70	5.71	0.809	1.50	15.28
6	12	600	30	20.00	0.333	0.76	6.64
7	16	200	70	2.86	0.905	10.81	110.75
8	16	400	30	13.33	0.555	1.03	9.92
9	16	600	50	12.00	0.600	0.67	6.52

Based on the experimental results of Table 2 it is deduced that there is a threshold of overlap beyond which the surface roughness rapidly increases. Namely, for overlap greater that 0.85 there is a significant increase in both Sa and Sz values. The parabolic increase trend of the surface roughness in respect to the overlap that it is depicted in Fig. 3, is in line with the respective literature [14].

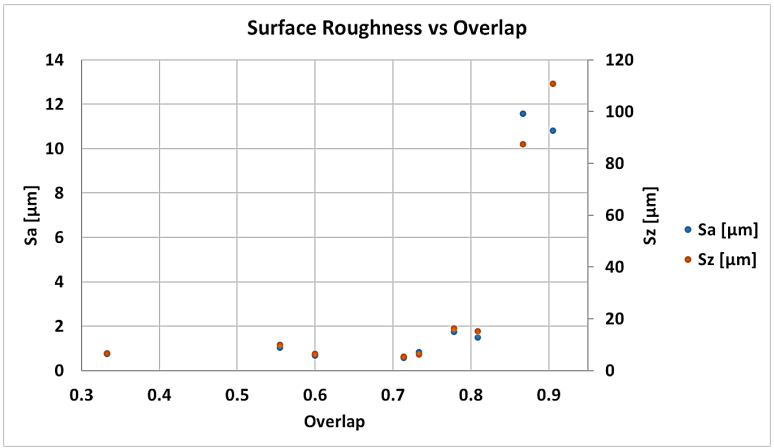

Fig. 3. Surface roughness values (Sa and Sz) in respect to the overlap.

In Fig. 4a and b, the main effects and interactions plots are depicted for Sa. At first, from the main effects plot it can be observed that although all parameters affect Sa, scanning speed causes the most significant variation of Sa values. More specifically, as the scanning speed increases, lower Sa is obtained, with the higher decrease of Sa values being noted between 200 and 400 mm/s. Thus, an appropriate selection of scanning speed values is crucial for achieving a high-quality surface during laser engraving process. Regarding the effect of mean power and pulse repetition frequency on Sa, it can be seen that they have a similar effect on Sa, as they both lead to an increase of average roughness up to a point and then the value of Sa remains almost constant.

Apart from the results presented in Fig. 4a, the interaction plots of Fig. 4b can also reveal more details about the combined effect of process parameters on Sa. Between mean power and scanning speed, a significant interaction is observed at the lowest value of scanning speed (200 mm/s), whereas for the other values of scanning speed, their interaction is negligible. However, the interaction of power and frequency is considerable for all levels of frequency, although a certain trend is not observed, as the correlation between power and frequency for each frequency level is different. Finally, the interaction between scanning speed and frequency is considerable only for the lowest value of frequency (30 kHz). Thus, it can be deduced that although power and frequency have a combined effect on the surface quality, the interaction between them and scanning speed is generally weak.

Various factors related to process parameters, such as the interaction time, overlap and energy per pulse contribute also to the creation of the surface topography. More specifically, if we consider the influence of scanning speed alone, with fixed values of mean power and pulse repetition frequency, due to the decrease of interaction time the heat-induced alterations of the surface are less intense, leading to improved surface roughness. As for mean power, when the other two parameters are fixed, the reason which leads to larger roughness is related to the larger thermal input to the workpiece, which leads to more intense thermal phenomena such as vaporization and remelting, which induce irregularities on the surface.

The effect of pulse repetition frequency, when scanning speed and power values are fixed, can be explained based on the interactions between various factors. More specifically, although the per pulse energy decreases, the hatching distance also decreases and the overlap increases. Thus, the higher number of repeated pulses, leading to a smaller overlap, creates a rougher surface with enlarged craters and other irregularities.

Finally, it can be deduced that, in order to avoid increased average roughness, lower power and frequency values should be used along with higher scanning speed values. However, these values should be selected taking also into consideration the effect of these parameters on the depth of produced pockets and the machining time, which are contradicting goals.

Afterwards, in order to be able to predict the roughness values in respect to process parameters for the specific material, an empirical relationship is established between process parameters and Sa. As a linear regression model was not able to describe the data with high correlation coefficient values, a power law model was adopted, as follows:

$$Sa = 151530 P^{0.354155} v_{scan}^{-2.70297} f^{0.920414} \quad (4)$$

The Mean Square Error (MSE) of the developed equation is 4.28060 μm^2 and the standard error of the regression (S) value is 2.06896 μm. The errors of the empirical equation can be attributed to the reduced number of experiments conducted when conducting the experiments with a DOE method like Taguchi method and some considerably high values occur. However, the choice of an established DOE method provided an excellent compromise between the cost of the experiments and the accuracy of the results.

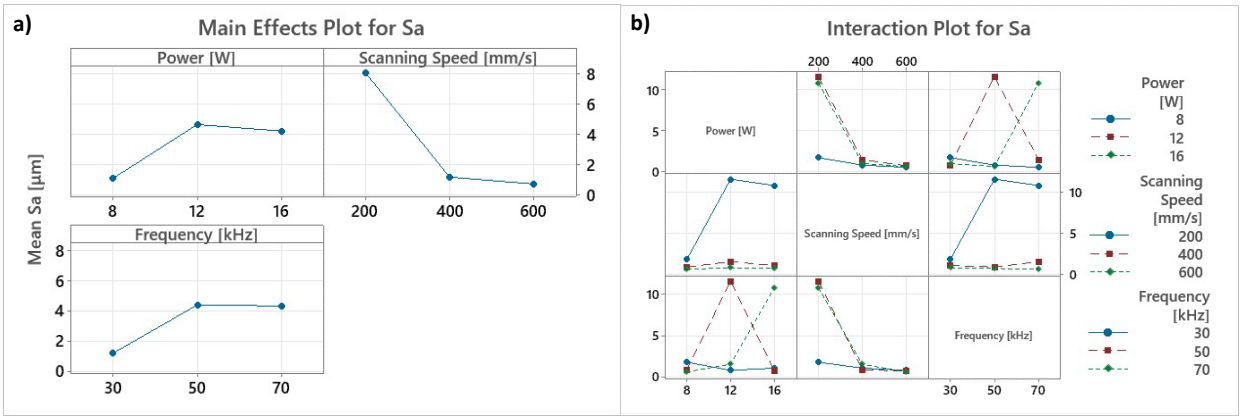

Fig. 4. (a) Main effects plot for Sa and (b) Interaction plot for Sa.

Regarding Sz values, the main effects plot of Figure 5a indicates that the three process parameters have a similar effect on Sz, as on Sa. Thus, it is shown that when laser scanning speed, which is again the most significant parameter, increases, the peak-to-valley height is considerably reduced for speed values up to 400 mm/s and then the decrease is slighter, whereas for both higher mean power and pulse repetition frequency, Sz increases more abruptly at first and then in a more gradual way. Moreover, the interactions plot of Figure 5b is also similar to that of Sa, indicating a higher degree of interaction between power and frequency, whereas the interaction between these parameters and scanning speed is weaker. An empirical relationship was also developed with a power law model with MSE value of 127.179 µm^2 and an S value of 11.2774 µm, in order to correlate the process parameters with Sz, as follows:

$$Sz = 197857 P^{0.818046} \upsilon_{scan}^{-2.52004} f^{0.859392} \quad (5)$$

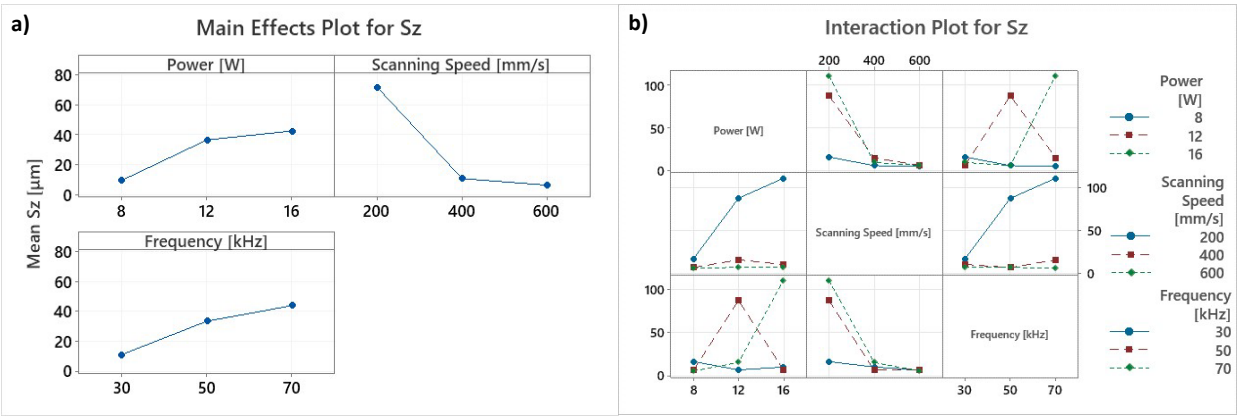

Fig. 5. (a) Main effects plot for Sz and (b) Interaction plot for Sz.

Summary

In this paper, the surface topography obtained during laser engraving of SAE304 is investigated by means of experimental work and statistical analysis. The experiment was designed based on Taguchi L9 orthogonal array for three levels of scanning speed, mean power and pulse repetition frequency in order to determine their effect on surface topography. After the results were analyzed, several conclusions were drawn:

Scanning speed considerably affects the surface topography, as indicated by the results of both Sa and Sz. For fixed mean power and pulse repetition rate, the decrease of interaction time between the laser beam and workpiece leads to lower heat input and less intense thermal phenomena, resulting in surfaces with higher quality and less irregular features.

Mean power and pulse repetition rate affect surface topography to a lower extent than scanning speed. As mean power increases, the heat input to the workpiece increases and a rougher surface is obtained as the more intense thermal phenomena lead to vaporization and remelting of the material and deeper microcraters are formed in the surface. Regarding pulse repetition rate, its increase leads to higher overlap and larger values of surface roughness. Thus, with regard to surface roughness, it is recommended that higher values of scanning speed and lower values of mean power and pulse repetition rate are desirable.

References

[1] Y.C. Shin, B. Wu, S. Lei, G.J. Cheng, Y.Y. Lawrence, Overview of Laser Applications in Manufacturing and Materials Processing in Recent Years, J. Manuf. Sci. Eng. Trans. 142 (2020) 110818. https://doi.org/10.1115/1.4048397

[2] P. Johander, I. Goenaga, D. Gomez, C. Moldovan, O. Nedelcu, P. Petkov, U. Kaufmann, H.J. Ritzhaupt-Kleissl, R. Dorey, K. Persson, Design and manufacturing of micro heaters for gas sensors, 4M 2006 - Second International Conference on Multi-Material Micro Manufacture (2006) pp. 117-121.

[3] E. Nikolidakis, A. Antoniadis, FEM modeling and simulation of kerf formation in the nanosecond pulsed laser engraving process, CIRP J. Manuf. Sci. Technol. 35 (2021) 236-249. https://doi.org/10.1016/j.cirpj.2021.06.014

[4] G. Schnell, U. Duenow, H. Seitz, Effect of Laser Pulse Overlap and Scanning Line Overlap on Femtosecond Laser-Structured Ti6Al4V Surfaces, Materials 13 (2020) 969. https://doi.org/10.3390/ma13040969

[5] K. Anderson, Aluminum Science and Technology, ASM International, 2018.

[6] S.L. Campanelli, G. Casalino, N. Contuzzi, Multi-objective optimization of laser milling of 5754 aluminum alloy, Opt. Laser Technol. 52 (2013) 48-56. https://doi.org/10.1016/j.optlastec.2013.03.020

[9] A. Pritam, Experimental investigation of laser deep engraving process for AISI 1045 Stainless Steel by Fibre Laser, Int. J. Inf. Res. Rev. 03 (2016) 1730-1734.

[10] P. Šugár, J. Šugárová, M. Frnˇcík, B. Ludrovcová, Nanosecond YB fibre laser milling of alluminium bronze: effect of process parameters on the surface finish, Adv. Sci. Technol. Res. J. 12 (2018) 10-15. https://doi.org/10.12913/22998624/93613

[11] N. Ahmed, S. Ahmad, S. Anwar, A. Hussain, M. Rafaqat, M. Zaindin, Machinability of titanium alloy through laser machining: material removal and surface roughness analysis, Int. J. Adv. Manuf. Technol. 105 (2019) 3303-3323. https://doi.org/10.1007/s00170-019-04564-7

[12] M.K. Mohammed, U. Umer, A.U. Rehman, Al-A.M. Ahmari, A.M. El-Tamimi, Microchannels fabrication in alumina ceramic using direct Nd: YAG Laser Writing, Micromachines 9 (2018) 371. https://doi.org/10.3390/mi9080371

[13] M.K. Mohammed, A. Al-Ahmari, Laser-machining of microchannels in NiTi-based shape-memory alloys: experimental analysis and process optimization, Materials 13 (2020) 2945. https://doi.org/10.3390/ma13132945

[14] H. Wan, J. Min, J. Lin, B.E. Carlson, S. Maddela, C. Sun, Effect of laser spot overlap ratio on surface characteristics and adhesive bonding strength of an Al alloy processed by nanosecond pulsed laser, J Manuf. Process. 62 (2021) 555-65. https://doi.org/10.1016/j.jmapro.2020.12.055